

## Gamma amplitudes are coupled to theta phase in human EEG during visual perception

Tamer Demiralp<sup>a,b,\*</sup>, Zubeyir Bayraktaroglu<sup>a</sup>, Daniel Lenz<sup>b</sup>, Stefanie Junge<sup>b</sup>, Niko A. Busch<sup>b</sup>, Burkhard Maess<sup>c</sup>, Mehmet Ergen<sup>a</sup>, Christoph S. Herrmann<sup>b</sup>

<sup>a</sup> *Istanbul University, Istanbul Faculty of Medicine, Department of Physiology, Turkey*

<sup>b</sup> *Department of Biological Psychology, Magdeburg University, Germany*

<sup>c</sup> *Max-Planck-Institute for Human Cognitive and Brain Sciences, Leipzig, Germany*

Received 20 May 2006; received in revised form 24 June 2006; accepted 13 July 2006

Available online 7 September 2006

### Abstract

Human subjects typically keep about seven items (plus or minus two) in short-term memory (STM). A theoretical neuronal model has been proposed to explain this phenomenon with physiological parameters of brain oscillations in the gamma and theta frequency range, i.e., roughly 30–80 and 4–8 Hz, respectively. In that model, STM capacity equals the number of gamma cycles (e.g., 25 ms for 40 Hz), which fit into one theta cycle (e.g., 166 ms for 6 Hz). The model is based on two assumptions: (1) theta activity should modulate gamma activity; and (2) the theta/gamma ratio should correlate with human STM capacity. The first assumption is supported by electrophysiological data showing that the amplitude of gamma oscillations is modulated by the phase of theta activity. However, so far, this has only been demonstrated for intracranial recordings. We analyzed human event-related EEG oscillations recorded in a memory experiment in which 13 subjects perceived known and unknown visual stimuli. The paradigm revealed event-related oscillations in the gamma range, which depended significantly on the phase of simultaneous theta activity. Our data are the first scalp-recorded human EEG recordings revealing a relationship between the gamma amplitude and the phase of theta oscillations, supporting the first assumption of the above-mentioned theory. Interestingly, the involved frequencies revealed a 7:1 ratio. However, this ratio does not necessarily determine human STM capacity. Since such a correlation was not explicitly tested in our paradigm, our data are not conclusive about the second assumption. Instead of theta phase modulating gamma amplitude, it is also conceivable that focal gamma activity needs to be downsampled to theta activity, before it can interact with more distant brain regions.

© 2006 Elsevier B.V. All rights reserved.

**Keywords:** Event-related oscillations; Phase; Time–frequency analysis

### 1. Introduction

In the past decades an increasing number of studies has described significant sensory-cognitive and motor correlates of brain oscillatory activity in different frequency ranges (Basar, 1980; Basar et al., 1999; Basar-Eroglu et al., 1992; Demiralp et al., 1999; Herrmann et al., 2004a,b; Klimesch et al., 1996). Based on these findings, Basar (2004) proposed that brain electrical oscillations reflect synchronous activation and communication

of selectively distributed neural networks that build dynamic assemblies responsible for specific perceptual or cognitive functions. The dynamic formation of such neuronal assemblies may range from local networks for early sensory processing to large-scale networks responsible for cognitive processes such as memory formation (Mesulam, 1994; Fuster, 1997).

EEG gamma oscillations (approx. 30–100 Hz) have been associated with multiple sensory and cognitive processes (Basar, 2004; Engel et al., 2001; Brosch et al., 2002). Especially memory functions are closely correlated with oscillations in the gamma band (Tallon-Baudry et al., 1998; Kaiser et al., 2003; Gruber et al., 2004; for a review, see Herrmann et al., 2004b). Also, theta oscillations have been found to be closely correlated with memory processes (Klimesch et al., 1996; Basar, 2004;

\* Corresponding author. Istanbul University, Istanbul Faculty of Medicine, Department of Physiology, Turkey. Tel./fax: +90 212 6352631.

E-mail address: [demiralp@istanbul.edu.tr](mailto:demiralp@istanbul.edu.tr) (T. Demiralp).

Jensen and Tesche, 2002). Therefore, it seems plausible to assume that the two oscillations interact during memory processes. Indeed, a theoretical model proposes that the number of items that can be held in short-term memory (STM) is equal to the number of gamma cycles that fit into one theta cycle (Lisman and Idiart, 1995). Typical gamma (e.g., 25 ms for 40 Hz) and theta activity (e.g., 166 ms for 6 Hz) yield values around 6.7, which are in the range of the ‘magical number seven’ (plus or minus two) that was suggested as the human STM capacity (Miller, 1956). However, so far, the model still requires support from human brain oscillations.

The interactions between different frequency ranges have been mainly observed in terms of the modulation of amplitudes of higher frequency oscillations by the phase of lower frequency oscillations in animal intracranial recordings (Steriade et al., 1996). Basar-Eroglu and Basar (1991) described a compound P300–40 Hz response in the cat hippocampus that may be the result of an interaction between delta oscillations mainly contributing to the P300 and the gamma oscillations. Especially in rodent hippocampus, the dependence of gamma amplitudes on the theta phase has been well characterized (Buzsaki and Draguhn, 2004). Later, Fell et al. (2005) have shown that successful target detection was associated with an increase of power and phase locking of hippocampal activity in both the low-frequency range and in the gamma range in intracranial recordings of epileptic patients. Mormann et al. (2005) found a task-dependent modulation of gamma activity by theta phase in the medial temporal lobes of epilepsy patients during a word recognition memory task. While most of these results on the gamma–theta coupling stem from mesial temporal structures, a recent study reports a modulation of the gamma amplitude by the theta phase in the sensory cortex. Lakatos et al. (2005) have simultaneously analyzed laminar profiles of current source densities and multiunit activity in the auditory cortex of macaques with implanted multi-contact electrodes and showed that theta amplitudes were modulated by delta phase and gamma amplitudes by theta phase.

All studies mentioned above are based on intracranial recordings of the local activity in human and animal subjects. Only a few studies on human scalp-recorded EEG have reported similar interrelations between gamma oscillations and lower frequencies. Schack et al. (2002) reported a coherence between the envelope of gamma activity at one electrode and theta activity at another electrode. In line with this observation, Burgess and Ali (2002) reported that the covariance of gamma activity across electrodes was modulated at theta frequency. However, neither of the two studies demonstrated a correlation of gamma *amplitude* with theta *phase* in a single location.

Therefore, we set out to analyze the amplitude of human EEG gamma activity with respect to the phase of the simultaneously occurring theta activity. Since the only example for coupling of human (intracranial) gamma amplitude and theta phase has been demonstrated in a memory paradigm (Mormann et al., 2005), we reanalyzed the data of a recent memory experiment which revealed clear gamma activity (Herrmann et al., 2004a).

## 2. Methods

### 2.1. Subjects

13 subjects (7 female) with a mean age of 25.4 (4.6 S.D.) years participated in the experiment. All subjects had normal or corrected-to-normal vision and showed no signs of any neurologic or psychiatric disorder. The experiment was conducted in line with local ethics guidelines.

### 2.2. Experiment

Subjects were presented line drawings of real-world objects for which they had representations in their long-term memory, and distorted versions of these drawings which could not be recognized. Objects and non-objects were matched for size and subtended visual angles of 5° to 10°. Sample stimuli are shown in Fig. 1.

The experiment was divided into one short practice block and two experimental blocks, each separated by a brief pause. The practice block contained 18 figures with 9 figures of each stimulus type. The experimental blocks included the remaining 192 figures (96 objects and 96 non-objects). The temporal sequence of stimuli was pseudo-randomized and equal for each subject. Each figure was shown for 1000 ms, followed by a randomized interstimulus interval of 1300–1700 ms, during which a black fixation cross was shown in the center of the screen.

Subjects were instructed to judge whether the stimuli appeared to be edgy or curvy by pressing one of two buttons. Thus, subjects were naive about the purpose of the experiment. At the end of the experiment, all subjects received a questionnaire to inquire demographic data as well as information about possible strategies used.

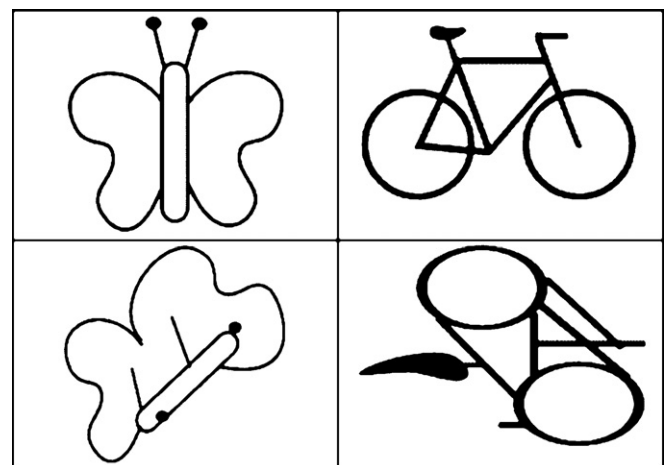


Fig. 1. Four examples of the stimuli used in the experiment. Top: for a butterfly (left) and a bicycle (right), subjects already have representations in their long-term memory. Bottom: For the distorted versions of these objects, no such memory representations exist. Objects in the left column were supposed to be judged as round objects while those in the right column were supposed to be judged as edgy.

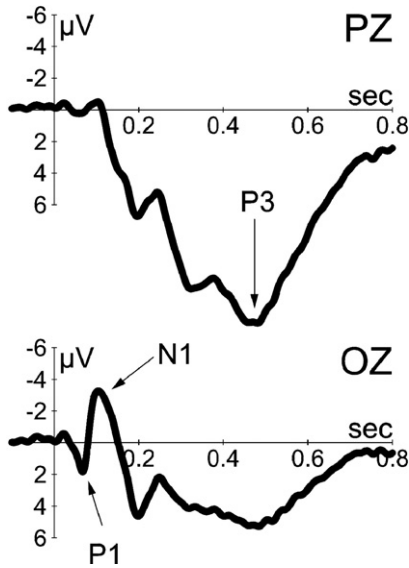


Fig. 2. Grand averages of the ERPs ( $N=13$ ) in midline parietal (upper trace) and occipital (lower trace) channels.

2.3. Data acquisition

Experiments were performed in a specially shielded cabin made of mu-metal, where usually magnetencephalograms (MEG) are recorded. No electric devices requiring AC power supply were operated inside the MEG cabin. Visual stimulation was provided by a Sony VPL X600E VGA projector which

projects the stimuli into the cabin via a mirror system. The projection plane was placed 60 cm in front of the subjects.

EEG was recorded with 52 Ag–AgCl electrodes mounted in an elastic cap (Quickcap) according to the international 10–10 system. All electrodes were referenced to the left mastoid and the ground electrode was placed at the right mastoid. The vertical electrooculogram (VEOG) was recorded by electrodes placed above and below the right eye, while the horizontal EOG (HEOG) was recorded from positions at the outer canthus of each eye. Electrode impedances were kept below 5 k $\Omega$ . Both EEG and EOG data were amplified using a Neuroscan amplifier with analog anti-aliasing filters set from DC to 100 Hz. Amplified EEG signals were sampled at 508.63 Hz by the MEG device (BTI Magnes WHS 2500) and stored on hard disk for off-line analysis. No MEG signals were recorded—we only used the MEG system because of the specially shielded cabin.

2.4. Data analyses

An automatic artefact rejection was applied to the continuous data, which excluded EEG segments when the standard deviation within a moving 200 ms time interval exceeded 50  $\mu$ V. The data were epoched between –500 and +1000 ms relative to stimulus onset and averaged to check the conformity of the obtained event-related potentials (ERPs) to visual perception experiments. In the present analyses, we pooled the potentials to both object and non-object stimuli to investigate gamma–theta coupling as a general phenomenon in visual perception.

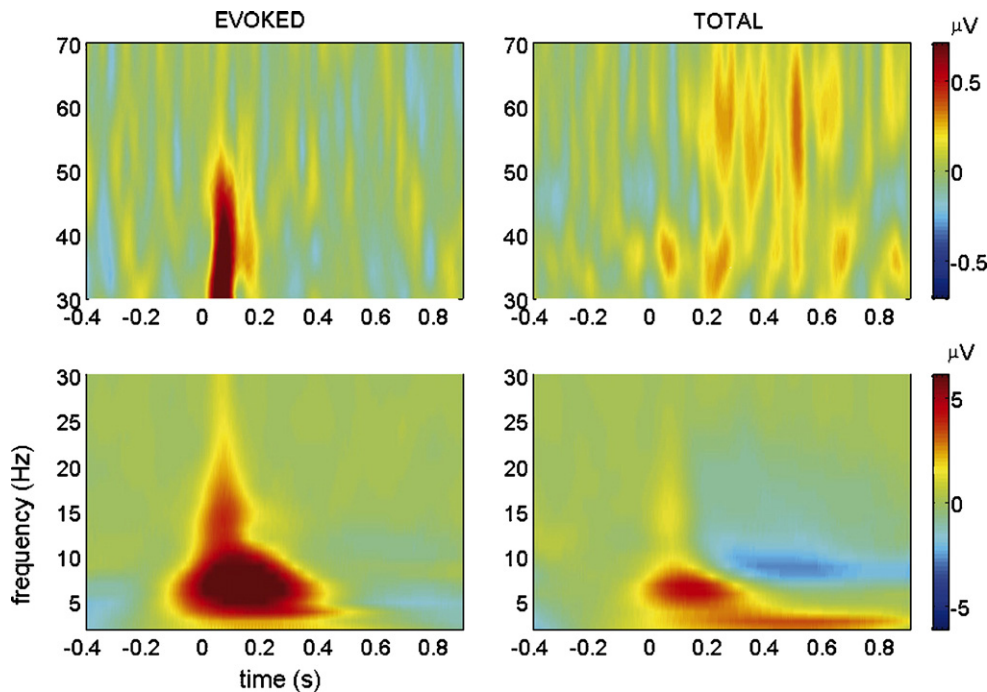


Fig. 3. Grand averages of the time–frequency transforms of the data for electrode O1 ( $N=13$ ). The upper row shows the gamma frequency range, while the lower row shows lower frequencies. Left column shows the evoked (phase-locked) activity and the right column displays the total activity (phase locked+non-phase locked). In both representations, the ongoing levels of oscillations were removed by subtracting mean amplitude of the –300 to –100 ms time window. Hence, only event-related changes in the time–frequency plane can be observed.

In order to analyze theta and gamma activity, a continuous wavelet transform (WT) with complex Morlet wavelets of 6 cycles was applied on single trials and on averaged ERP. The magnitudes of the WTs of single trials were subsequently averaged to obtain the total activity, which includes signal components that are phase-locked or non-phase-locked to the triggering event, whereas magnitudes of the WT of the averaged ERP were computed to obtain the evoked activity that reflects only phase-locked signal components. For each scale of the WT a baseline correction was applied using the mean amplitude within the  $-300$  to  $-100$  ms time window.

Since the visual stimulation evoked maximal gamma responses over occipital electrodes (cf. Fig. 4), we focussed on the O1 electrode for further analyses. Individual gamma and theta frequencies of each subject were determined using the total activity at the O1 electrode. The peaks of both theta and gamma activity were determined in the first 300 ms after stimulus onset and in the 4–7 Hz and 30–80 Hz frequency bands, respectively. If no clear peak was visible in the gamma-range, 40 Hz was chosen for analysis. This had to be done for four subjects.

From this stage on, only the WTs in individual theta and gamma frequencies were analyzed. The mean gamma frequency of all subjects was 40.1 Hz and mean theta frequency was 5.9 Hz.

The dependence of gamma amplitudes upon theta phase was analyzed using a similar approach as that used by Lakatos et al. (2005) for spontaneous EEG. The phase of theta activity was extracted from the WTs of single trials for every sampling point. The relation between the theta phase and gamma amplitude was analyzed in two time windows: 0–300 ms and 500–800 ms. For this purpose, the phase values of the theta oscillations of all sampling points in all single trials were concatenated to form one single series of data points for each subject and for each of the two time windows. The same procedure was also carried out for the gamma amplitudes. Next, all data points whose theta phases fall in one of the 60 phase intervals of  $\pi/30$  width between  $-\pi$  and  $\pi$  were identified and assigned to this phase interval. By this procedure, the data points were sorted in ascending order into 60 phase intervals (cf. Fig. 5, top). Then, the mean gamma amplitudes of the

respective data points were assigned to each theta phase interval. Thus, the gamma amplitudes in single trials were sorted according to 60 theta phase intervals. Gamma amplitudes sorted according to this method were used to visualize our results (cf. Fig. 5 middle row).

### 2.5. Statistical analyses

For statistical analyses the 60 sorted gamma amplitudes of each subject were further sub-sampled by a factor of 10 to obtain 6 mean gamma amplitudes for theta phase intervals of  $\pi/3$  between  $-\pi$  and  $\pi$  (cf. Fig. 5, bottom). The significance of the differences of gamma amplitudes among these 6 theta phase intervals was statistically tested using a repeated-measures ANOVA with the theta phase as the within-subject factor with 6 levels. Greenhouse–Geisser correction was applied to the degrees of freedom, with corrected probability values reported.

## 3. Results

### 3.1. Behavioural data

There were no significant differences between the reaction times in response to object and non-object stimuli, but for edgy versus curvy objects due to the use of the dominant hand for responses to edgy and of the non-dominant hand for responses to curvy objects ( $F(1,12)=10.7$ ;  $p<0.05$ ). In the present analyses we pooled the single trials to both object and non-object stimuli to investigate gamma–theta coupling as a general phenomenon in visual perception.

### 3.2. ERP

After artifact rejection, mean number of sweeps analyzed per subject was 140. Fig. 2 displays the ERPs recorded in electrodes Oz and Pz averaged over 13 subjects. ERPs were averaged across object and non-object trials. The ERPs show the typical waveform for visual perception experiments with P1–N1 waves dominantly expressed in the occipital region and a large P3 wave in the parietal region.

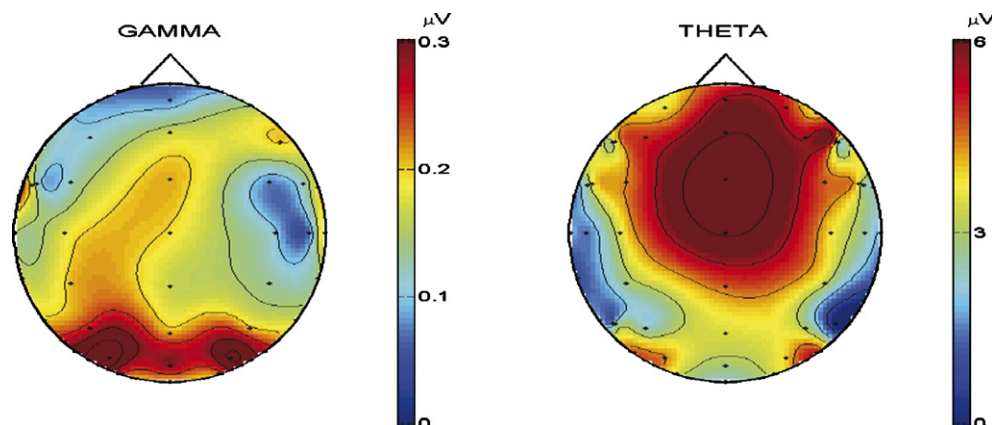


Fig. 4. Topographies of the maxima of the total gamma and total theta amplitudes within the first 300 ms. The plots are based on the grand average of 13 subjects. Total gamma activity shows a typical occipital distribution, whereas total theta activity shows a midline frontal maximum with two bilateral local maxima at occipital area.

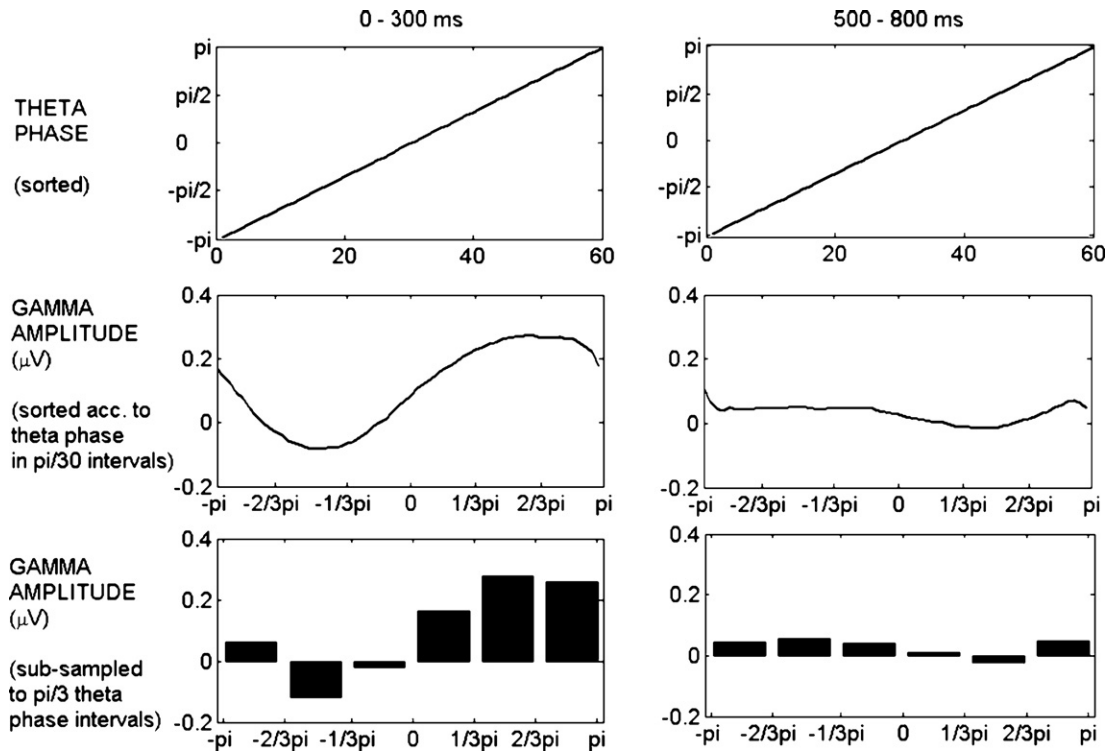


Fig. 5. Grand average of the sorted mean theta phases within  $\pi/30$  intervals (upper row). Grand average of the gamma amplitudes (middle row) and sub-sampled gamma amplitudes (lower row) sorted according to the theta phase. The left column shows the results obtained for the early (0–300 ms) and the right column for the late time window (500–800 ms). For the early time window (0–300 ms), the gamma amplitudes were significantly larger during positive theta phases compared with those occurring during negative theta phases ( $F(5,60)=8.28$ ;  $p<0.002$ ) with a maximum at  $2/3\pi$  and a minimum at  $-2/3\pi$ , whereas no significant difference was found among the gamma amplitudes at different theta phases in the late time window.

### 3.3. Time–frequency transforms

Fig. 3 demonstrates the grand averages of the time–frequency transforms of the data from electrode O1. An earlier report on the data focussed on the strong evoked gamma response in the early time window in the occipital area (Herrmann et al., 2004a,b) and reported a significant increase of the evoked gamma response to objects compared with those to non-objects. In the total gamma activity on the right upper plot, however, in addition to the early gamma component later gamma packets can also be observed, which last up to 800 ms. The strongest contribution of the low frequency range in O1 stems from the theta band in the first 300 ms as seen in both evoked and total activity.

Total gamma activity had an occipital maximum in the first 300 ms time interval (cf. Fig. 4, left), similar to the topography of evoked gamma activity reported by Herrmann et al. (2004a). The maximum amplitude of total theta activity within the same time window revealed a midline frontal maximum with two bilateral local maxima at the occipital area. Therefore, we focussed on the relationship between the theta phase and gamma amplitude in the occipital region.

Gamma amplitudes of early (0–300 ms) and late (500–800 ms) time windows of all single trials were sorted according to the simultaneously occurring theta phase with a resolution of  $\pi/30$ , and differences among the gamma amplitudes at different theta phases were investigated (Fig. 5, middle row).

For statistical analyses, the gamma amplitudes sorted according to theta phase were sub-sampled to obtain mean gamma amplitudes for 6 theta phase intervals of  $\pi/3$  width each. Repeated-measures ANOVA applied on the gamma amplitudes in these 6 theta phase intervals yielded a significant difference among the gamma amplitudes for the early time window (0–300 ms:  $F(5,60) = 8.35$ ;  $p<0.003$ ), but not for the late time window (500–800 ms:  $F(5,60) = 0.42$ , NS). The within-subject contrasts showed that the significant differences in the early time window stemmed from the significantly lower amplitudes in second and third phase intervals ( $p<0.01$  and  $p<0.05$ , respectively) and significantly higher amplitudes in the fifth and sixth phase intervals ( $p<0.002$  and  $p<0.007$ , respectively) compared with the mean gamma amplitude in all 6 phase ranges, with a maximum at  $2/3\pi$  and a minimum at  $-2/3\pi$  (Fig. 5, left column, lower row).

## 4. Discussion

Our analysis revealed that the amplitude of event-related gamma oscillations in human EEG correlates significantly with the phase of simultaneously occurring theta oscillations. Thus, our data are in line with the idea that such gamma–theta coupling could be important for understanding the STM capacity as proposed by Lisman and Idiart (1995). However, since we did not investigate EEG activity while subjects hold items in STM, the gamma–theta coupling seems to be a more

general phenomenon, and it seems plausible to assume that it occurs also during other perceptual and cognitive processes.

Interestingly, the relation of theta and gamma frequencies in our paradigm was roughly 5.9 Hz to 40.1 Hz. Thus, the gamma oscillations were about seven times faster than the modulatory theta rhythm. However, this is not surprising, because dividing the theta wavelength by the gamma wavelength will by definition of these frequency bands result in a number close to 7. This number may vary across subjects, but would only be meaningful if it correlated with a behavioural memory measure. According to the theory by [Lisman and Idiart \(1995\)](#) memory capacity is determined by the number of gamma cycles which fit into one theta cycle. If this gamma–theta model of STM, which is indirectly supported by our results, were true, subjects with slow theta or fast gamma rhythms would have larger memory span. This, however, remains to be demonstrated.

Our data seem to support the notion that gamma activity is modulated by the theta phase ([Lakatos et al., 2005](#)). However, our results do not exactly resemble the ones of that study, which is based on the measurement of current source densities in the auditory cortex of macaques with implanted multi-contact electrodes. While [Lakatos et al. \(2005\)](#) correlated the gamma amplitude and theta phase of spontaneous oscillations, we observed such correlations in event-related oscillations. In addition, the correlation was only evident during the first 300 ms after stimulation but not during the later time interval. This difference might be due to the spatial extent of the signals measured with both techniques. The spontaneous gamma–theta coupling observed in the local circuits with intracranial measurements might not be observable in the scalp recordings because of the superimposition of a wide range of theta and to a lesser extent gamma oscillations from neighboring structures due to spatial smearing in surface recordings. However, as more specific and local generators would be responsible for the event-related activity, the event-related gamma and theta oscillations might stem from a more local and more specific network, in which they interact with each other.

The presence of the observed coupling between event-related theta and event-related gamma oscillations raises the question about which is the cause and which is the effect. On the one hand, this relationship can be explained by a resetting of the theta phase through gamma generators. On the other hand, a modulation of the gamma amplitude by the ongoing theta phase in terms of a preferred phase of theta oscillation that facilitates gamma bursting could be the underlying mechanism. A further, alternative explanation of our data could be a reset of gamma and theta oscillations by stimulation ([Makeig et al., 2002](#)), which would result in a temporary correlation of the two rhythms. Of course, it is also possible that theta and gamma oscillations do not interact directly. Instead, a third process could have triggered both gamma and theta rhythms or might have served as an interface between the two. This question needs to be addressed in future studies.

The first two of the above-mentioned mechanisms could have important implications for theories on information processing. It has been proposed that the gamma rhythm probably serves to build local patches of synchrony, whereas lower

frequency oscillations are more robust for the establishment of long-distance interactions ([Von Stein and Sarnthein, 2000](#); [Varela et al., 2001](#)). Therefore, beyond the topology and spatial coherence within one frequency range as usually analyzed in EEG-ERP studies, the dynamic interactions among the oscillations in different frequency bands becomes an important field of research for the understanding of how activations of local networks may be transferred or translated to large-scale networks (bottom–up integration) and how at the same time large-scale networks may control the activations in more local circuitry (top–down integration).

[Basar \(2004\)](#) hypothesized that superimposed oscillations during cognitive processes reflect the activity of multiple selectively distributed networks working in parallel, which are responsible for different levels of processing during the formation of specific object representations in memory. Our results on the gamma–theta coupling might extend this superposition principle in terms of an interaction or cross-talk mechanism between these different networks that represent different processing levels. While gamma activity was found very localized over occipital cortex, theta activity was more widespread including frontal cortex. This makes sense from a theoretical point of view: Since gamma is assumed to reflect local processing, gamma activity alone would not suffice for the communication of all brain structures responsible for the perception of and reaction to a stimulus. This requires a long-range interaction as offered by theta activity. A downsampling from local occipital gamma to local occipital theta seems to be a first step followed by propagation of theta to frontal cortex. A similar downsampling mechanism across frequencies has been suggested previously for the interaction of distant brain regions ([Basar, 2004](#); [Chen and Herrmann, 2001](#)).

Although the causality and the exact mechanism of the relationship between gamma and theta oscillations is not certain at the current stage, our findings show that interactions between oscillators acting in different frequency bands can be observed in human scalp recordings during information processing.

## Acknowledgement

This study was supported by the Alexander von Humboldt Stiftung grant to Tamer Demiralp, Research Fund of Istanbul University Project No. UDP 229/18022004 and Grants DFG-HE 3353/2 and SFB/TR-31 to CSH.

## References

- Basar, E., 1980. EEG-Brain Dynamics: Relation between EEG and Brain Evoked Potentials. Elsevier, Amsterdam.
- Basar, E., 2004. Memory and Brain Dynamics: Oscillations Integrating Attention, Perception, Learning, and Memory. CRC press, Boca Raton.
- Basar, E., Demiralp, T., Schurmann, M., Basar-Eroglu, C., Ademoglu, A., 1999. Oscillatory brain dynamics, wavelet analysis, and cognition. *Brain Lang.* 66 (1), 146–183.
- Basar-Eroglu, C., Basar, E., 1991. A compound P300–40 Hz response of the cat hippocampus. *Int. J. Neurosci.* 60 (3–4), 227–237.
- Basar-Eroglu, C., Basar, E., Demiralp, T., Schurmann, M., 1992. P300-response: possible psychophysiological correlates in delta and theta frequency channels. A review. *Int. J. Psychophysiol.* 13 (2), 161–179.

- Brosch, M., Budinger, E., Scheich, H., 2002. Stimulus-related gamma oscillations in primate auditory cortex. *J. Neurophysiol.* 87 (6), 2715–2725.
- Burgess, A.P., Ali, L., 2002. Functional connectivity of gamma EEG activity is modulated at low frequency during conscious recollection. *Int. J. Psychophysiol.* 46 (2), 91–100.
- Buzsaki, G., Draguhn, A., 2004. Neuronal oscillations in cortical networks. *Science* 304, 1926–1929.
- Chen, A.C.N., Herrmann, C.S., 2001. Perception of pain coincides with the spatial expansion of human EEG dynamics. *Neurosci. Lett.* 297 (3), 183–186.
- Demiralp, T., Yordanova, J., Kolev, V., Ademoglu, A., Devrim, M., Samar, V.J., 1999. Time–frequency analysis of single-sweep event-related potentials by means of fast wavelet transform. *Brain Lang.* 66 (1), 129–145.
- Engel, A.K., Fries, P., Singer, W., 2001. Dynamic predictions: oscillations and synchrony in top–down processing. *Nat. Rev., Neurosci.* 2 (10), 704–716.
- Fell, J., Kohling, R., Grunwald, T., Klaver, P., Dietl, T., Schaller, C., Becker, A., Elger, C.E., Fernandez, G., 2005. Phase-locking characteristics of limbic P3 responses in hippocampal sclerosis. *Neuroimage* 24 (4), 980–989.
- Fuster, J.M., 1997. Network memory. *Trends Neurosci.* 20, 451–459.
- Gruber, T., Tsvilivis, D., Montaldi, D., Muller, M.M., 2004. Induced gamma band responses: an early marker of memory encoding and retrieval. *Neuroreport* 15 (11), 1837–1841.
- Herrmann, C.S., Lenz, D., Junge, S., Busch, N.A., Maess, B., 2004a. Memory-matches evoke human gamma-responses. *BMC Neurosci.* 13 (5), 13.
- Herrmann, C.S., Munk, M.H., Engel, A.K., 2004b. Cognitive functions of gamma-band activity: memory match and utilization. *Trends Cogn. Sci.* 8 (8), 347–355.
- Jensen, O., Tesche, C.D., 2002. Frontal theta activity in humans increases with memory load in a working memory task. *Eur. J. Neurosci.* 15 (8), 1395–1399.
- Kaiser, J., Ripper, B., Birbaumer, N., Lutzenberger, W., 2003. Dynamics of gamma-band activity in human magnetoencephalogram during auditory pattern working memory. *Neuroimage* 20 (2), 816–827.
- Klimesch, W., Doppelmayr, M., Russegger, H., Pachinger, T., 1996. Theta band power in the human scalp EEG and the encoding of new information. *Neuroreport* 7 (7), 1235–1240.
- Lakatos, P., Shah, A.S., Knuth, K.H., Ulbert, I., Karmos, G., Schroeder, C.E., 2005. An oscillatory hierarchy controlling neuronal excitability and stimulus processing in the auditory cortex. *J. Neurophysiol.* 94 (3), 1904–1911.
- Lisman, J.E., Idiart, M.A., 1995. Storage of 7±2 short-term memories in oscillatory subcycles. *Science* 267 (5203), 1512–1515.
- Makeig, S., Westerfield, M., Jung, T.P., Enghoff, S., Townsend, J., Courchesne, E., Sejnowski, T.J., 2002. Dynamic brain sources of visual evoked responses. *Science* 295, 690–694.
- Mesulam, M.M., 1994. Neurocognitive networks and selectively distributed processing. *rev. Neurol. Paris* 150 (8–9), 564–569.
- Miller, G.A., 1956. The magical number seven plus or minus two: some limits on our capacity for processing information. *Psychol. Rev.* 63 (2), 81–97.
- Mormann, F., Fell, J., Axmacher, N., Weber, B., Lehnertz, K., Elger, C.E., Fernandez, G., 2005. Phase/amplitude reset and theta-gamma interaction in the human medial temporal lobe during a continuous word recognition memory task. *Hippocampus* 15, 890–900.
- Schack, B., Vath, N., Petsche, H., Geissler, H.G., Moller, E., 2002. Phase-coupling of theta-gamma EEG rhythms during short-term memory processing. *Int. J. Psychophysiol.* 44 (2), 143–163.
- Steriade, M., Contreras, D., Amzica, F., Timofeev, I., 1996. Synchronization of fast (30–40 Hz) spontaneous oscillations in intrathalamic and thalamocortical networks. *J. Neurosci.* 16, 2788–2808.
- Tallon-Baudry, C., Bertrand, O., Peronnet, F., Pernier, J., 1998. Induced gamma-band activity during the delay of a visual short-term memory task in humans. *J. Neurosci.* 18 (11), 4244–4254.
- Varela, F., Lachaux, J.P., Rodriguez, E., Martinerie, J., 2001. The brainweb: phase synchronization and large-scale integration. *Nat. Rev., Neurosci.* 2 (4), 229–239.
- von Stein, A., Sarnthein, J., 2000. Different frequencies for different scales of cortical integration: from local gamma to long range alpha/theta synchronization. *Int. J. Psychophysiol.* 38 (3), 301–313.